Synthesis of Block and Graft Copolymers with Linear Polyethylene Segments by Combination of Degenerative Transfer Coordination Polymerization and Atom Transfer Radical Polymerization

Hiromu Kaneyoshi, Yoshihisa Inoue, and Krzysztof Matyjaszewski*

Center for Macromolecular Engineering, Department of Chemistry, Carnegie Mellon University, 4400 Fifth Avenue, Pittsburgh, Pennsylvania 15213

Received February 4, 2005; Revised Manuscript Received May 10, 2005

ABSTRACT: Block and graft copolymers with polyacrylate and linear polyethylene segments were synthesized through a combination of degenerative transfer (DT) ethylene polymerization and atom transfer radical polymerization (ATRP). DT coordination polymerization was mediated by a bis(imino)-pyridineiron/diethylzinc binary catalyst system activated by MAO and was studied at various temperatures. The catalyst system achieved a well-controlled DT coordination polymerization of ethylene, resulting in low-polydispersity polyethylene with high chain end functionality. The Zn-terminated polyethylene prepared by DT coordination polymerization was oxidized using dry air, followed by hydrolysis to provide a monohydroxy-terminated polyethylene (PE-OH). The degree of ethylene polymerization (DP $\sim$ 20) and the chain end functionality ($\sim$80%) of PE-OH were determined by ^{1}H NMR. The PE-OH was converted into a polyethylene α-bromoisobutyrate macroinitiator (PE-MI), and ATRP of *n*-butyl acrylate and *tert*-butyl acrylate was successfully conducted from the PE-MI to produce well-defined block copolymers. A PE-*block*-P*n*BA copolymer (M_n = 10 100, M_w/M_n = 1.16 with 7.4 wt % PE segment) and a PE-*block*-P*t*BA copolymer (M_n = 11 000, M_w/M_n = 1.16 with 6.8 wt % PE segment) were obtained successfully. The α-bromoisobutyrate/PE-MI was dehydrobrominated to form a polyethylene macromonomer with a terminal α-methacrylate group (PE-MM). A grafting-through ATRP was performed with the PE-MM and either *n*-butyl acrylate or *tert*-butyl acrylate to form well-defined P*n*BA-*graft*-PE and P*t*BA-*graft*-PE copolymers. Molecular structures were determined by ^{1}H NMR and GPC analysis. The P*t*BA-*graft*-PE was hydrolyzed yielding PAA-*graft*-PE with 90% carboxylic acid functionality. DSC analysis of the graft copolymers indicated two separate glass transitions, suggesting phase-separated morphology.

Introduction

Coordination olefin polymerization has been extensively investigated since the discovery of Ziegler/Natta catalysis in the 1950s.[1,2] This resulted in polyolefins being the largest volume commodity polymers in the world and indispensable to our lifestyle. After the historical discoveries by Ziegler and Natta, the chemists in this field mainly directed their interest at enhancement of catalyst activity, incorporation of comonomers into the polymers, and development of catalysts that allow stereoregular polymerization in a controlled fashion.[3] These investigations led to the discovery of highly active homogeneous single-site metallocene[4−6] and post-metallocene catalysts[7−14] that offered good control over tacticity and enabled a high degree of comonomer incorporation. A new category of coordination olefin polymerization, namely living coordination olefin polymerization, has rapidly developed in the past decade.[11,15−21] Several specific single-site catalysts limit chain transfer and termination reactions in olefin polymerization, provide metal-terminated living polyolefin copolymers with high chain end functionality, and allow architectural control over new polyolefin materials, including the preparation of chain end functionalized polyolefins and polyolefin-based block copolymers.[22−25]

However, a disadvantage of these catalysts is their ability to produce only one living polymer chain per metal center. This drives up the cost of the catalyst and limits its industrial impact. One solution to this problem would be the development and use of chain transfer reagents. A number of functional polyolefin chains could be produced from one metal center using this technique. In fact, several chain transfer olefin polymerization systems are already known, including those using chain transfer agents such as boron,[26] silicon,[27] zinc,[28] and aluminum[29] compounds, and they provide chain end functionalized polyolefins.[30,31] However, the rate constant of chain transfer to these agents was usually low, and excess chain transfer reagents had to be used in order to increase chain transfer efficiency. Furthermore, the chain transfer reactions were irreversible and, therefore, the levels of control over molecular weight and molecular weight distribution were almost the same as in nonliving olefin polymerization systems.

In the same time frame, several controlled/"living" radical polymerization processes (CRP) have been developed. Three different CRP[32−35] mechanisms have been extensively studied (Scheme 1). The first mechanism involves spontaneous reversible homolytic cleavage of a dormant chain end (eq 1) and is exemplified by nitroxide-mediated polymerizations[36] or cobalt-mediated systems.[37] The second one is based on a catalytic reversible homolytic cleavage of a covalent bond via a redox process (eq 2), which occurs in atom transfer radical polymerization (ATRP).[38−41] The third process is based on a thermodynamically neutral bimolecular exchange between growing radicals and a dormant species. Degenerative transfer (DT) with alkyl iodides[42] and reversible addition−fragmentation chain transfer (RAFT) belong in this category.[43] Our motivation in this study was to adapt this third mechanism to coordination olefin polymerization.

* Corresponding author. E-mail: km3b@andrew.cmu.edu.

10.1021/ma050263j CCC: $30.25
Published on Web 06/04/2005

Scheme 1. Three General Mechanisms for Controlled/ "Living" Radical Polymerization

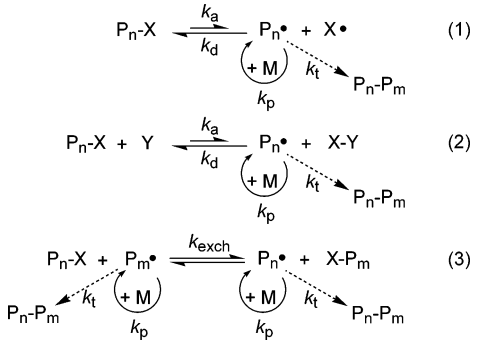

Scheme 2. General Mechanism for Degenerative Transfer Coordination Olefin Polymerization

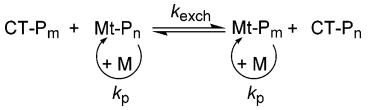

In the case of the above-mentioned chain transfer olefin polymerization, if there was a large difference in the thermodynamic energy between the alkyl complex with the active catalyst (Mt-P_n) and with the chain transfer reagent (CT-P_m), or if the activation energy of the exchange reaction in Scheme 2 were too high, the chain transfer reaction would be irreversible. Consequently, control over the polymerization would be close to that seen in a nonliving polymerization. However, if the thermodynamic energies of Mt-P_n and CT-P_m were sufficiently close and the activation energy of the alkyl exchange reaction was significantly lower, then the chain transfer reaction could occur quickly and reversibly. Indeed, this mechanism is very similar to degenerative transfer (DT) radical polymerization. The resulting polyolefin should have controlled molecular weight and molecular weight distribution. A further advantage of this DT system is that one active catalyst metal center could produce hundreds of living polymer chains.

In fact, several ethylene polymerization catalyst systems behave essentially like a DT olefin polymerization, e.g., the combination of actinocene/trialkylaluminium,[44,45] lanthanocene/dialkylmagnesium,[46] half-sandwich chromocene/trialkylaluminium,[47−49] bis(imino)pyridineiron/dialkylzinc,[50,51] and zirconocene/zirconocene.[52] Limitation of these catalyst systems is either high cost of chain transfer agent or the low molecular weight of the resulting polyethylene. Since the linear polyethylene formed in the reactions possess both high crystallinity and poor solubility in the solvent at the reaction temperature, the polymers separate from the polymerization media, and control is lost after certain a conversion is reached. Therefore, controlled polymerization could only be conducted to a low degree of polymerization (<100) with these catalyst systems. In this paper, we focus on a bis(imino)pyridineiron/diethylzinc catalyst system described recently in detail by Gibson[50,51] that provides efficient DT polymerization of ethylene. We also discuss procedures for functionalization of zinc-terminated polyethylene and the syntheses of block and graft copolymers with linear polyethylene segments via ATRP.

Experimental Section

Characterization. The molecular weight and molecular weight distribution of the linear polyethylenes were measured by high-temperature gel permeation chromatography using a Waters 150-C GPC equipped with three Tosoh TSK-GEL columns (two sets of TSKgelGMH_{HR}-H(S)HT and one TSKgel-GMH_6-HTL) at 145 °C. GPC was performed using *o*-dichlorobenzene as eluent at a flow rate of 1 mL/min. Linear polystyrene standards were used for calibration. ^{1}H NMR spectra of the chain end functional polyethylenes and molecular weight and structure of the block and graft copolymers were examined in toluene-d_8 at 80 °C, deuterated chloroform at 30 °C, and/or tetrahydrofuran-d_8 at 30 °C using a Bruker 300 MHz spectrometer. Conversion of *n*-butyl acrylate and *tert*-butyl acrylate monomer were determined by gas chromatography using a Shimadzu GC 14-A gas chromatograph equipped with a FID detector and J&W Scientific 30 m DB WAX Megabore column. Anisole was used as an internal standard. Molecular weight and molecular weight distribution of the block and graft copolymers were measured by gel permeation chromatography with PSS columns (styrogel 10^5, 10^3, 10^2 Å) and RI detector. GPC was performed using THF as eluent at a flow rate of 1 mL/min. Molar mass of the block and graft copolymers were determined relative to linear polystyrene calibration standards. Differential scanning calorimetry data for graft copolymers were obtained using Seiko SSC/5200 instrument. In the case of the P*n*BA-*graft*-PE, the following scanning temperature program was used. First, the temperature was cooled from room temperature to −150 °C and kept at this temperature for 3 min. Next, the temperature was increased to 170 °C at the rate of 10 °C/min, maintained for 3 min, and then cooled to −150 °C at the rate of −20 °C/min, where it was maintained for another 3 min. This heating and cooling process was conducted three times, and data from the third heating cycle were adopted. In the case of P*t*BA-*graft*-PE and PAA-*graft*-PE, the scanning temperature program was similar to that of P*n*BA-*graft*-PE, except for the maximum temperature (180 °C) and minimum temperature (−20 °C).

Materials. Ethylene was purchased from PRAXAIR, Inc. Air was dried by passing through a calcinated molecular sieves column. Methylaluminoxane (MAO) was purchased from Aldrich as a 10 wt % toluene solution. The remaining trimethylaluminum was removed under vacuum before use, and the residue was redissolved in *o*-xylene. Diethylzinc was purchased from Aldrich as a 1.0 M toluene solution. The bis(imino)pyridine−iron dichloride complex[10] was prepared according to the literature procedure. Toluene (Fisher Scientific, >99%) was distilled over sodium/benzophenone and degassed with nitrogen. *o*-Xylene (Aldrich, anhydrous grade), 2-bromo-2-methylpropionyl bromide (Acros, 98%), and 1,8-diazabicyclo[5.4.0]-undec-7-ene (DBU; Acros, 98%) were used without purification. Triethylamine (Acros, 99%) was dried over potassium hydroxide and degassed with nitrogen prior to use.

Copper(I) bromide (Acros, 98%) was purified according to the previous report.[53] Tris(2-(di(2-(*n*-butoxycarbony)ethyl)-amino)ethyl)amine (BA_6TREN)[54] and tris((*N*,*N*-dimethylamino)ethyl)amine (Me_6TREN)[55] were prepared as detailed in previous reports. *n*-Butyl acrylate (*n*BA; Acros, >99%) and *tert*-butyl acrylate (*t*BA; Aldrich, 98%) were passed through a neutral alumina column to remove stabilizer, dried over calcium hydride, distilled under reduced pressure, and degassed with nitrogen. Methyl 2-bromopropionate (MBP; Aldrich, 98%) was dried over molecular sieves. Chlorobenzene (Acros, >99%) was dried over molecular sieves and degassed with nitrogen. Dichloromethane (Fisher Scientific, >99%) was distilled over calcium hydride. All other reagents were used as received.

Degenerative Transfer Coordination Ethylene Polymerization. The bis(imino)pyridine−iron complex (3.0 mg, 5×10^{-6} mol) was added under a nitrogen blanket to a 500 mL round-bottom flask equipped with a magnetic stirring bar and dissolved in *o*-xylene (25 mL). After warming to the desired temperature, the catalyst solution was saturated by bubbling ethylene through the solution for 10 min. Then, 0.2 M MAO in *o*-xylene (2.5 mL, 5×10^{-4} mol) and 1.1 M $ZnEt_2$ in toluene (proper amounts relative to the iron complex) were added to the solution to start polymerization. During the polymerization, the ethylene pressure was kept over 1 atm. After the

Table 1. Conditions and Results for Degenerative Transfer Ethylene Polymerization Using Bis(imino)pyridine−Iron/$ZnEt_2$ Catalyst at Various Temperatures[a]

run	$ZnEt_2$ (equiv)	temp (°C)	time (min)	yield (g)	activity (g/(mmol h))	M_n[b]	$M_{n,th}$[c]	M_w[b]	M_w/M_n[b]
1	0	25	30	1.979	800	62600		319800	5.11
2	500	25	30	2.653	1080	230	500	290	1.28
3	20	80	30	0.672	130	1700	1700	2200	1.32
4	10	100	30	0.118	20	560	1200	970	1.75

[a] Polymerization conditions: *o*-xylene (50 mL), 5 μmol of Fe complex, 100 equiv of MAO, 1 atm ethylene. [b] GPC data based on PS standard calibration. [c] $M_{n,th}$ = [polymer yield (g)]/[$ZnEt_2$ amount (mol)]/2.

desired polymerization time, the reaction was stopped by the addition of concentrated aqueous HCl. The resulting mixture was poured into excess methanol, and the precipitated polyethylene was filtered, washed with methanol, and dried at 60 °C under vacuum.

Synthesis of Monohydroxy-Terminated Polyethylene (PE-OH). *o*-Xylene (3 mL), $ZnEt_2$ (2.3 mL, 2.5×10^{-3} mol), and MAO (0.3 mL, 5×10^{-4} mol) were placed in a 25 mL Schlenk flask equipped with a magnetic stirring bar under nitrogen. Separately, ethylene gas was bubbled through a solution of the bis(imino)pyridine−iron complex (3.0 mg, 5×10^{-6} mol) in *o*-xylene (50 mL) stirring at room temperature. After 10 min, the $ZnEt_2$/MAO mixed solution was added to this solution to start polymerization. After 30 min the remaining ethylene gas was purged from the reaction by bubbling nitrogen through the reaction, and then the polymerization mixture was warmed to 100 °C. Dry air was bubbled into the mixture at this temperature for 2 h. After the oxidation reaction was complete the mixture was poured into acidic methanol (500 mL) to precipitate the PE-OH. The white powder was filtered, washed with methanol, and then dried under vacuum at 60 °C. Yield 2.11 g.

Synthesis of a Polyethylene Macroinitiator (PE-MI) for ATRP. PE-OH (1.78 g, chain end functionality 77%, 2.3×10^{-3} mol) was placed into a Schlenk flask (250 mL) equipped with a magnetic stirring bar, and then the flask was evacuated and backfilled with nitrogen three times. Toluene (120 mL) was added to this flask, and the mixture was stirred for 30 min at 100 °C. Et_3N (2.0 mL, 14.3×10^{-3} mol) was added to the solution followed by 2-bromo-2-methylpropionyl bromide (1.5 mL, 11.9×10^{-3} mol), and the reaction was stirred for 1 h at 100 °C. After the reaction mixture was cooled to room temperature, it was poured into methanol (850 mL). The resulting insoluble pale brown powder was collected through filtration, washed with methanol, and dried under vacuum at 80 °C. The PE-MI was obtained as a pale brown solid. Yield 1.88 g.

Synthesis of a Polyethylene Macromonomer (PE-MM). The PE-MI (1.48 g, chain end functionality 69%, 1.38×10^{-3} mol) was placed in a Schlenk flask (250 mL) equipped with a magnetic stirring bar, and then the flask was evacuated and backfilled with nitrogen three times. Toluene (70 mL) was added, and this mixture was allowed to warm to 60 °C with stirring. DBU (20 mL, 0.131 mol) was added to this mixture and stirring continued for 24 h at 60 °C. After the reaction mixture was cooled to room temperature it was poured into methanol (700 mL). The insoluble pale brown powder was filtered, washed with methanol and THF, and dried at 60 °C under reduced pressure. PE-MM was obtained as pale brown solid. Yield 1.29 g.

ATRP of *n*BA and *t*BA from a PE-MI. A typical ATRP was performed as follows using standard Schlenk techniques. Solvent, an internal standard, and monomers were degassed through bubbling with nitrogen for 30 min prior to use. A stock solution of catalyst was prepared by dissolving CuBr (44.8 mg, 3.13×10^{-4} mol), $CuBr_2$ (3.9 mg, 1.75×10^{-5} mol), and BA_6-TREN (335.3 mg, 3.66×10^{-4} mol) in chlorobenzene (2.5 mL). Separately, the PE-MI (111 mg, 1.03×10^{-4} mol of Br) was placed in a 25 mL Schlenk flask equipped with a magnetic stirring bar, and then the flask was evacuated and backfilled with nitrogen three times. Chlorobenzene (1.0 mL), anisole (0.2 mL), BA (1.5 mL, 1.02×10^{-2} mol), and catalyst stock solution (0.82 mL, 1.40×10^{-4} mol of CuBr/BA_6TREN, 6.98×10^{-6} mol of $CuBr_2$/BA_6TREN) were successively added to this flask. The resulting mixture was heated to 100 °C to start the polymerization. The PE-MI dissolved in the polymerization medium within a few minutes. Samples were taken via a syringe periodically to follow the kinetics of the polymerization process. The samples were diluted with THF followed by filtration through a neutral alumina column and a Gelman Acrodisc 0.2 μm PTFE filter prior to analysis by gas chromatography (GC) and gel permeation chromatography (GPC). After polymerization, the resulting deep green solution was poured into methanol (100 mL), and the insoluble solid was collected by filtration and washed with methanol. The residual solid was mixed with acetone (20 mL), and the acetone-soluble material was separated from the mixture by filtration and then passed through a Gelman Acrodisc 0.2 μm PTFE filter. After evaporation, the acetone-soluble material was dried at 80 °C under vacuum for 2 h.

Table 2. Results for ATRP with Polyethylene Macroinitiator (PE-MI)[a]

no.	monomer	time (h)	conv (%)	M_n[b] $\times 10^{-4}$	$M_{n,th}$[c] $\times 10^{-4}$	M_w[b] $\times 10^{-4}$	M_w/M_n[b]
1	*n*BA	8	72.8	1.03	1.01	1.19	1.16
2	*t*BA	6	80.5	1.04	1.11	1.20	1.16

[a] Polymerization conditions: $[BA]_0/[PE\text{-}MI]_0/[CuBr]_0/[CuBr_2]_0/[BA_6TREN]_0$ = 100/1/1/0.05/1.05, $[BA]_0$ = 2.93 mol/L; solvent = chlorobenzene (1.8 mL); initiator = polyethylene macroinitiator (M_n = 750); temperature = 100 °C. [b] GPC data were based on PS standard calibration. [c] $M_{n,th}$ was calculated based on the conversion of BA measured by GC.

Grafting-Through ATRP of the PE-MM with *n*BA and *t*BA. A typical ATRP (run 2 in Table 3) was conducted using standard Schlenk techniques. The solvent, internal standard, and monomers were degassed through bubbling with nitrogen for 30 min prior to use. Me_6TREN (1.8×10^{-3} mL, 6.83×10^{-6} mol) was placed in a Schlenk flask equipped with a magnetic stirring bar and cooled in a liquid nitrogen bath. CuBr (1.1 mg, 7.68×10^{-6} mol) and PE-MM (328 mg, 3.37×10^{-4} mol) were added to this flask, and then the flask was evacuated and backfilled with nitrogen three times. *n*BA (1.5 mL, 1.02×10^{-2} mol) and anisole (0.2 mL) were added to this mixture, and then the resulting mixture was stirred at room temperature for 30 min. Dichlorobenzene (3.3 mL) and MBP (3.8×10^{-3} mL, 3.41×10^{-5} mol) were successively added to the flask, and then the flask was heated to 100 °C to start polymerization. Samples were taken via a syringe periodically to follow the kinetics of the polymerization process. The samples were diluted with tetrahydrofuran followed by filtration through a neutral alumina column and a Gelman Acrodisc 0.2 μm PTFE filter prior to analysis by gas chromatography (GC) and gel permeation chromatography (GPC). After 3 h, the polymerization mixture was poured into methanol (150 mL), and then the insoluble white solid was filtered off and washed with methanol. The resulting solid was extracted with acetone (100 mL) to remove any unreacted PE-MM from the graft copolymer. After evaporation of solvent, the residual solid was dried at 60 °C under vacuum. P*n*BA-*g*-PE was obtained as a pale yellow solid.

Hydrolysis of P*t*BA-*graft*-PE. The P*t*BA-*g*-PE copolymer (102 mg, 7.0×10^{-4} mol for *t*Bu ester group) was placed in a Schlenk flask equipped with a magnetic stirring bar, and then the flask was evacuated and backfilled with nitrogen three times. Dichloromethane (2 mL) was added to the flask, and the slurry was stirred at room temperature to dissolve the graft

Table 3. Copolymerization Conditions and Analytical Results for PBA-*graft*-PE via ATRP[a]

no.	BA	ligand	$[M]_0/[PE\text{-}MM]_0/[I]_0/[CuBr]_0/[L]_0$	time (h)	BA conv[b] (%)	M_n(GPC)[c] $\times 10^{-4}$	M_n(NMR)[d] $\times 10^{-4}$	M_w/M_n[c]	DP of BA/PE-MM[d]
1	*n*BA	BA_6TREN	300/5/1/1/1	21	77.1	2.57	2.02	1.39	140/3.1
2	*n*BA	Me_6TREN	300/10/1/0.2/0.2	3	69.3	2.24	2.75	1.34	190/4.5
3	*t*BA	Me_6TREN	300/5/1/0.3/0.3	7	75.2	2.35	2.55	1.39	181/3.3
4	*t*BA	Me_6TREN	300/10/1/0.4/0.4	4	80.5	3.06	2.69	1.27	184/4.7

[a] Polymerization conditions: $[BA]_0 = 2.05$ mol/L; solvent = chlorobenzene/anisole (3.3 mL/0.2 mL); initiator = methyl 2-bromopropionate; temperature = 100 °C. [b] Determined by GC. [c] GPC data were based on PS standard calibration, and M_n were determined after fractionation. [d] Calculated based on ^{1}H NMR study.

Scheme 3. Reaction Mechanism for Degenerative Transfer Ethylene Polymerization in a Bis(imino)pyridine−Iron/Dialkylzinc Binary Catalyst System

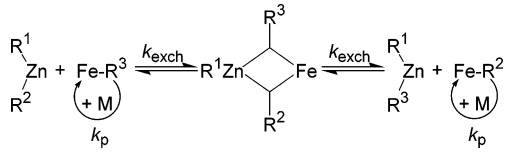

copolymer. Then, trifluoroacetic acid (0.27 mL, 3.50×10^{-3} mol) was added to this solution, and the mixture was stirred at room temperature for 15 h. The solvent was removed from the resulting heterogeneous mixture by decantation, and the residual solid was washed with dichloromethane (3 mL × 3) followed by drying under vacuum at room temperature for 6 h. PAA-*graft*-PE was obtained as white solid. Yield 70 mg.

Results and Discussion

Degenerative Transfer Coordination Ethylene Polymerization. The polymerization of ethylene in the presence of a bis(imino)pyridineiron/diethylzinc binary catalyst system was recently discussed in detail by Gibson et al.[51] It was proposed that the catalyst resting state is a bimetallic complex which dissociates into a free coordinatively unsaturated iron organometallic species (Scheme 3). This species can either propagate via ethylene insertion or associate with any available dialkylzinc species. Chain growth via monomer insertion occurs only on iron species. Alkyl groups on zinc (including polyethylene chains) exchange degeneratively with alkyl groups on iron. Thus, dialkylzinc species does not react directly with ethylene. If the exchange process (dissociation/association) is sufficiently fast in comparison with propagation, polyethylene with low polydispersity is formed. Therefore, the essence of the process is the degenerative transfer.

The kinetics, the dependence of degree of polymerization, and polydispersity on conversion for the DT polymerization, when contribution from other side reactions is negligible, are represented as[56]

$$R_p = k_p[M][Mt] \quad (1)$$

$$DP_n = \Delta[M]/([Mt]_0 + [CT]_0) \quad (2)$$

$$M_w/M_n = 1 + (2/p - 1)(2k_p/k_{exch}) \quad (3)$$

In an ideal case, as illustrated in Scheme 2, the degree of polymerization increases linearly with conversion, and it is predetermined by the combined concentration of the active catalyst (Mt) and the chain transfer agent (CT) added to the reaction. (For dialkylzinc, after cleavage of the Zn−C bond, its concentration should be multiplied by two.) The polydispersity index decreases with conversion, p, and depends on the ratio of rate constants of propagation and exchange reactions (eq 3).

Scheme 4. Molecular Structure of Bis(imino)pyridine−Iron Complex

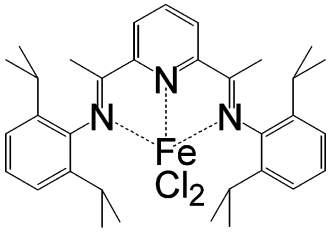

However, in practice, the poor solubility of the resulting linear polyethylene at ambient temperature limits the application of these ideal laws. Precipitation of active and dormant polymer species from the reaction medium strongly reduces the magnitude of k_{exch} and results in the formation of uncontrolled polymers. Therefore, control of molecular weights and polydispersities for polyethylene was observed only for relatively low degrees of polymerization (<100).[50,51] One possible solution to this problem is to increase the solubility of linear polyethylene by increasing the polymerization temperature. Therefore, DT ethylene polymerization at higher temperatures was attempted using the bis(imino)-pyridine−iron catalyst (Scheme 4) and diethylzinc in order to achieve higher molecular weight polyethylene in a controlled fashion.

Ethylene polymerization was conducted in the presence of a bis(imino)pyridine−iron complex activated with methylaluminoxane and $ZnEt_2$ at various temperatures, and the results are summarized in Table 1. When ethylene polymerization was conducted at 25 °C without $ZnEt_2$, high molecular weight polyethylene with high polydispersity index was obtained. When 500 equiv of $ZnEt_2$, compared to the iron catalyst, was added to this reaction system, the GPC trace of the resulting polymer showed a sharp monomodal peak, and polydispersity was significantly lower ($M_w/M_n = 1.28$), similar to that reported previously.[50,51] The large deviation of GPC molecular weight from the theoretical value was due to linear polystyrene used as the standard calibration.

The polymerization temperature was raised to 80 °C in order to dissolve higher molecular weight linear polyethylene while retaining control over the polymerization. However, the catalytic activity of the Fe complex dramatically decreased with increasing reaction temperature, presumably due to decomposition of active species and lower solubility of ethylene gas in the polymerization medium. Because of this lower activity of the Fe catalyst, the amount of $ZnEt_2$ added to the reaction was reduced to 20 equiv against the iron catalyst. As presented in Figure 1, the GPC trace of the resulting polyethylene shifted toward the higher molecular weight region, and the number-average molecular weight was ≈7 times larger than that of the polyethylene obtained at 25 °C. Extension of polymer-

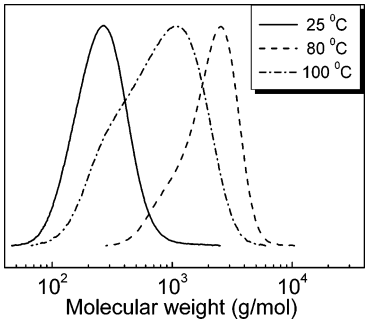

Figure 1. GPC traces for polyethylene produced by DT coordination ethylene polymerization using bis(imino)pyridine−iron/$ZnEt_2$ catalyst at various temperatures. See Table 1 for polymerization conditions.

ization time did not increase the degree of polymerization, presumably due to thermal decomposition of active species. The polydispersity index remained low (M_w/M_n = 1.32) although a low molecular weight shoulder peak was noticeable. Therefore, while the polymerization at 80 °C was still feasible, the contribution of side reactions, including other chain transfer reactions and catalyst decomposition, was more pronounced. To further enhance the solubility of the formed polyethylene, the polymerization was conducted at 100 °C. Polymerization activity was strongly reduced due to thermal decomposition of active species. Therefore, only 10 equiv of $ZnEt_2$ to Fe catalyst was added in order to obtain higher molecular weight polyethylene. However, even with lower amounts of $ZnEt_2$ the molecular weight of the polyethylene was lower than that obtained at 80 °C. The polydispersity index was fairly high (M_w/M_n = 1.75), and shoulder peaks appeared in the GPC trace, indicating other side reactions.

In conclusion, although control over polymerization was limited, at higher temperatures DT coordination ethylene polymerization led to higher molecular weight polyethylene. However, at higher temperatures, catalytic activity of the bis(imino)pyridineiron/diethylzinc catalyst system decreased and contribution of other side reactions increased. Nevertheless, other metallocene and post-metallocene catalysts that operate at high temperature should be tested in combination with other transfer agents to extend the range of molecular weights of well-defined polyolefins prepared by degenerative transfer.

Preparation of Hydroxy-Terminated Polyethylene (PE-OH) from Zinc-Terminated Polyethylene. The bis(imino)pyridineiron/diethylzinc catalyst system allowed the preparation of a well-defined di(polyethylenyl)zinc with low polydispersity index by DT coordination ethylene polymerization at 25 °C. This di(polyethylenyl)zinc was used for synthesis of end-functionalized polyethylenes. The alkyl−zinc bond can be oxidized by oxygen and subsequently hydrolyzed in situ to form a hydroxy-terminated polyethylene (PE-OH). The reaction procedure is illustrated in Scheme 5. After conducting the DT coordination ethylene polymerization at 25 °C, the resulting di(polyethylenyl)zinc was oxidized by exposure to dry air at 100 °C to form di(polyethylenoxy)zinc. This reaction was performed at high temperature in order to better dissolve the di(polyethylenyl)zinc in *o*-xylene. The reaction medium immediately turned homogeneous after heating to 100 °C. After the oxidation reaction was complete, the resulting di(polyethylenoxy)zinc was poured into acidic methanol to provide

Scheme 5. Reaction Pathway for the Synthesis of Hydroxyl-Terminated Polyethylene (PE-OH)

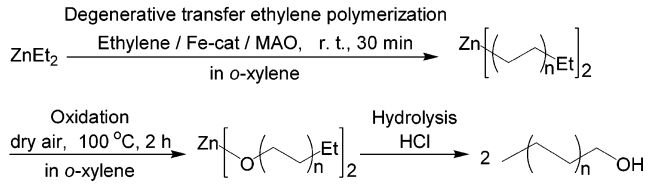

hydroxy-terminated polyethylene (PE-OH). Extending the oxidation reaction time beyond 2 h resulted in the production of peroxides.

The molecular structure of the PE-OH was confirmed by ^1H NMR (Figure 2). No peaks attributable to chain

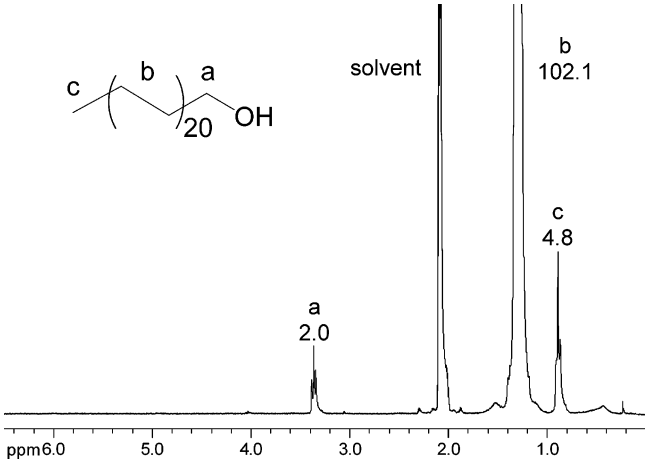

Figure 2. ^1H NMR spectrum of hydroxy-terminated polyethylene (PE-OH) in toluene-d_8 at 80 °C (300 MHz).

end vinyl protons were observed between 4.5 and 6.5 ppm, suggesting that other chain transfer reactions such as β-hydrogen transfer reaction to metal or monomer did not occur in the DT coordination ethylene polymerization conducted at 25 °C. Methine protons, which would indicate presence of a branched polyethylene, were not observed; therefore, the polyethylene segment should have a linear structure. The presence of a triplet peak (−CH_2OH, δ = 3.4 ppm, peak *a*), which can be assigned to methylene protons next to an oxygen atom, indicated that the oxidation proceeded successfully. Therefore, the chain end functionality of PE-OH was estimated by comparison of the integrals of this triplet and a triplet (−CH_3, δ = 0.9 ppm, peak *c*) that can be assigned to the methyl protons at the other end of PE-OH chain. The integral ratio of triplets was 2/4.8 although the ideal ratio should be 2/3. The difference between 3 and 4.8 indicated the presence of some unfunctionalized polyethylene (PE). The PE content was calculated on the basis of the assumption that this sample was a mixture of PE-OH and PE with linear polyethylene segment. The ratio of a chain end methyl group in PE-OH to PE was 3 to 0.9 (= (4.8 − 3)/2). Therefore, the chain end functionality of PE-OH was determined to be 77% (= 3/(3 + 0.9)). The loss of functionality can occur during the DT process or during oxidation and hydrolysis. If oxidation is carried out with moist air, almost no PE-OH is formed. Regardless, various methods for drying air did not produce PE-OH with functionality higher than 77%.

The M_n of the PE-OH was determined by comparison of integrals of the triplet peak at 3.4 ppm (I_{CH_2O} = 2) with the singlet peak for the methylene protons (−CH_2−,

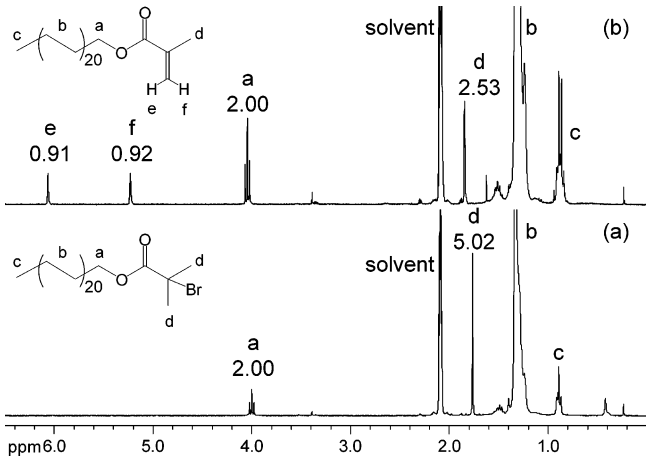

Figure 3. 300 MHz ^{1}H NMR spectra of (a) α-bromoisobutyrate-terminated polyethylene (PE-MI) and (b) methacryloyl-terminated polyethylene (PE-MM) in toluene-d_8 at 80 °C.

$\delta = 1.3$ ppm, peak b, $I_{CH_3} = 102$). The methylene protons contain signals from both methylene peaks in PE-OH and in PE. On the basis of the 77% functionality, the real integral of methylene protons in PE-OH was estimated to be 78.6 (= 102 × 0.77). Since this integral value (78.6) should correspond to the multiples of the four protons present in an ethylene monomer, the degree of polymerization of ethylene in the PE-OH was determined to be 19.7 (= 78.6/4). This number would be an average degree of polymerization, and the calculated M_n of PE-OH is ≈600. An elemental analysis of PE-OH showed a range of 82.80−83.08 wt % C and 14.15−14.20 wt % H, whereas values of 82.97 wt % C and 14.27 wt % H were expected from the calculation based on M_n and functionality calculated from ^{1}H NMR.

Synthesis of a Polyethylene Macroinitiator (PE-MI) for ATRP from PE-OH. The terminal OH functionality present on the PE-OH can be used to introduce other functionality through conventional organic reactions, such as α-haloester group to initiate ATRP. Thus, the hydroxyl group on PE-OH was converted into the α-bromoisobutyrate group by the reaction with excess 2-bromo-2-methylpropionyl bromide in the presence of triethylamine in toluene at 100 °C. As shown in Figure 3a, the ^{1}H NMR spectrum of the resulting product revealed the presence of a triplet peak for the methylene protons next to an oxygen atom (−CH_2O−, $\delta = 4.0$ ppm, peak a) and singlet peak for methyl protons in the ester group (−(CH_3)$_2$Br, $\delta = 1.8$ ppm, peak d). The integral of the singlet ($I_{CH_3} = 5.02$) was relatively smaller than triplet ($I_{CH_2O} = 2.00$); the ideal ratio should be $I_{CH_3}/I_{CH_2O} = 6/2$. This difference may be due to the different sensitivity of each proton caused by the aggregation of α-bromoisobutyrate-terminated polyethylene (a polyethylene macroinitiator, PE-MI) under this measurement condition and of some relaxation time differences between end group protons. However, the absence of a triplet peak (−CH_2OH, $\delta = 3.4$ ppm, peak a in Figure 2) and the presence of an another triplet signal (−CH_2O−, $\delta = 4.0$ ppm, peak a in Figure 3a) proved that esterification of PE-OH proceeded quantitatively. The negligible small peaks at 3.4 ppm may be methoxy group in methoxy-terminated polyethylene produced by etherification of PE-OH and methanol. Thus, the esterification product was composed of a mixture of PE-MI and unfunctionalized linear polyethylene. The chain end functionality of the PE-MI, calculated on the basis of the same methodology used in the case of PE-OH (the comparison of integrals of peaks a, b, and c), was 69%. The calculated M_n of PE-MI was 750.

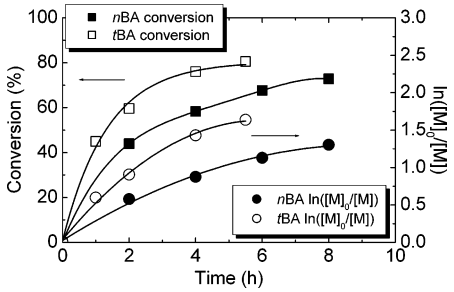

Figure 4. Kinetic plots of polymerization of nBA and tBA from the PE-MI at 100 °C.

Synthesis of a Polyethylene Macromonomer (PE-MM) from the PE-MI. The direct reaction between the PE-OH and methacryloyl chloride was accompanied by formation of side products with methylenoxy group, even under mild reaction conditions. Therefore, the methacryloyl ester functionality was introduced by dehydrobromination of the α-bromoisobutyrate group. Dehydrobromination was conducted on the PE-MI with excess 1,8-diazabicyclo[5.4.0]undec-7-ene (DBU) in toluene at 60 °C for 24 h. DBU is an efficient dehydrobromination reagent even under mild reaction conditions.[57] The molecular structure and NMR spectrum of the resulting compound are shown in Figure 3b. The appearance of two new multiple peaks (=CH_2, δ = 5.2 and 6.1 ppm, peaks e and f), which are characteristic of vinylidene protons in a methacrylate group, supported the formation of a methacrylate-terminated polyethylene (polyethylene macromonomer, PE-MM). A triplet peak assignable to methylene protons bonding to an oxygen atom (−CH_2O−, $\delta = 4.1$ ppm, peak a) and a singlet peak from the methyl protons in a methacrylate group (−C(=CH$_2$)CH_3, $\delta = 1.8$ ppm, peak d) were slightly shifted downfield to those in the parent PE-MI. No peaks originating from methyl groups in the isobutyrate moiety of PE-MI were observed. The proportion of the integrals of e, f, a, and d peaks (0.91, 0.92, 2.00, and 2.53) should be similar difference as before (1/1/2/3). These results prove that the α-bromoisobutyrate group was converted into a methacrylate group without side reactions. Accordingly, the resulting compound consisted of the PE-MM and nonfunctional linear polyethylene. The chain end functionality of the reaction product was calculated using the same method used in the case of the PE-OH (the comparison of integrals of peaks a−c) and determined to be 68%. The calculated M_n of PE-MM was 660.

Preparation of Polyethylene-*block*-poly(butyl acrylate)s via ATRP. ATRP of n- and $tert$-butyl acrylate initiated by PE-MI was conducted with CuBr/CuBr$_2$/BA$_6$TREN as a catalyst and chlorobenzene as a solvent. BA$_6$TREN is an efficient ligand for the incorporation of PE segments for ATRP in nonpolar media because of the good solubility of the copper complex in chlorobenzene, a solvent for PE-MI, and the resulting block copolymer at elevated temperatures. 5% of CuBr$_2$ relative to CuBr was added to the reaction system to provide additional control over the polymerization. The results of two polymerizations are presented in Table 2. In the case of nBA polymerization, the conversion of nBA reached 72.8% in 8 h, although the first-order kinetic plots exhibited a gradual curvature (Figure 4).

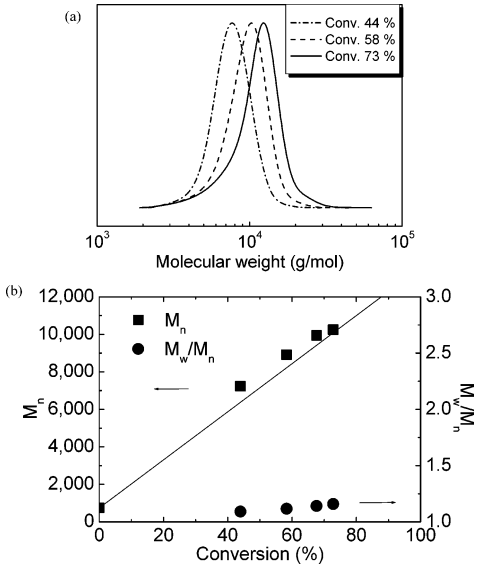

Figure 5. (a) GPC traces and (b) the evolution of M_n and M_w/M_n as a function of *n*BA conversion for polymerization of *n*BA from the PE-MI at 100 °C.

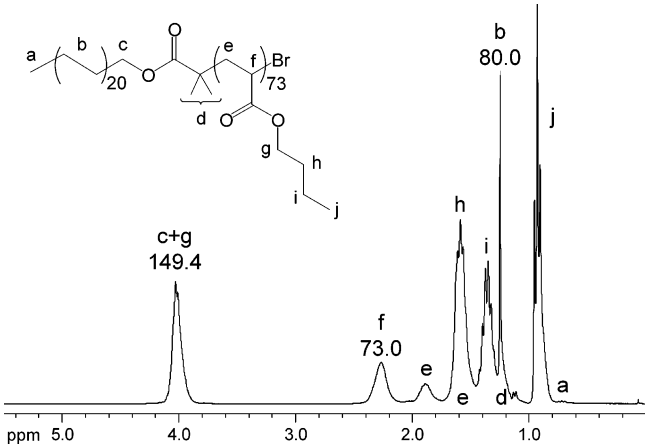

Figure 6. ^{1}H NMR spectrum of PE-*block*-P*n*BA in $CDCl_3$ at 30 °C (300 MHz).

The evolution of molecular weight of the block copolymer was investigated by GPC analysis (Figure 5a). The GPC traces shifted toward the high molecular weight region, and all peaks had a sharp monomodal shape, indicating that the PE-MI was an efficient initiator. No peaks for nonfunctional linear polyethylene were appeared in GPC traces because of the complete separation by filtration after THF extraction. As shown in Figure 5b, the M_n of the block copolymer increased linearly with *n*BA conversion, and the values were close to the theoretical ones. The molecular weight distribution remained quite narrow ($M_w/M_n < 1.2$). These results demonstrate that the chain extension reaction from the α-bromoisobutyrate group in a PE-MI proceeded successfully, and a well-defined block copolymer was formed.

After polymerization, fractionation of the final sample by acetone was carried out in order to remove polyethylene present in the PE-MI. The acetone-soluble polymer was collected after filtration, and then the molecular structure of the residual polymer was examined by ^{1}H NMR study in $CDCl_3$ (Figure 6). The spectrum revealed that a singlet peak ($-CH_2-$, $\delta = 1.25$ ppm, peak *b*) from the polyethylene segment and typical poly(*n*BA) peaks were present in this sample. The degree of polymerization of the poly(*n*BA) segment was estimated by comparison of the integration of the relevant peaks. When the integral of the polyethylene segment (peak *b*) was 80 (80 methylene protons in PE-MI, $DP_{PE} = 20$), the integral of methine protons in *n*BA (peak *f*) was 73. Thus, the degree of polymerization of poly(*n*BA) was $DP_{nBA} = 73$. This value is in a good agreement with the number calculated on the basis of the *n*BA conversion measured by GC ($DP_{nBA} = 72.8$ in Table 2). The integral of the $-CH_2O-$ group in *n*BA and PE-MI (peak $c + g$, $I = 74.7 = 149.4/2$) agrees with this value. Accordingly, the total molecular weight of PE-*block*-P*n*BA was $M_n = 10\,100$, and the weight ratio of polyethylene segment was 7.4%.

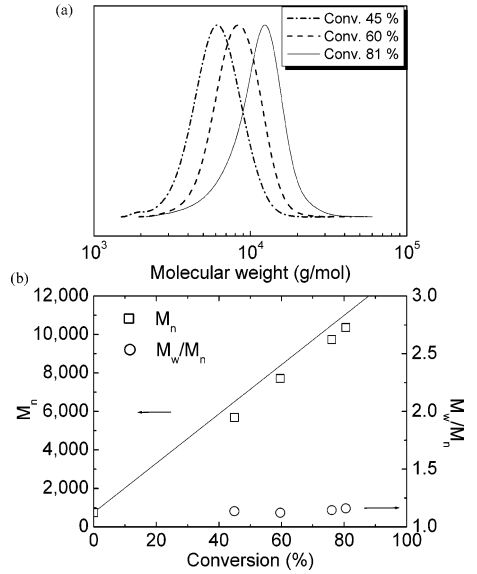

Figure 7. (a) GPC traces and (b) the evolution of M_n and M_w/M_n as a function of *t*BA conversion for polymerization of *t*BA from the PE-MI at 100 °C.

For *t*BA block copolymerization, conversion of *t*BA reached 80.5% in 6 h, as shown in Table 2. The polymerization proceeded a little faster than that of *n*BA, and the first-order kinetic plots also showed some curvature (Figure 4). The evolution of molecular weight was investigated by GPC analysis (Figure 7a). GPC revealed that traces from all samples had monomodal shapes, and these curves shifted progressively toward the higher molecular weight region with *t*BA conversion. As mentioned above, nonfunctionalized polyethylenes were successfully removed from the sample by filtration after THF extraction. The M_n of the block copolymer increased linearly with *t*BA conversion (Figure 7b). The deviation from the theoretical line was insignificant, indicating that chain propagation reaction from PE-MI was well controlled. The polydispersity index was low ($M_w/M_n < 1.2$), as for *n*BA. Fractionation of the final sample using acetone was performed, and the molecular structure of acetone-soluble polymer was investigated by ^{1}H NMR analysis in $CDCl_3$ (Figure 8). As expected, a singlet peak ($\delta = 1.25$ ppm, peak *b*) for methylene protons in a polyethylene segment and peaks attributed to poly(*t*BA) could be observed. The degree of polymerization of *t*BA in the block copolymer was calculated using the same method as for the PE-*block*-P*n*BA and the value determined $DP_{tBA} = 80$. This value agrees with the number calculated from the GC data (80.5 in Table 2). Therefore, the calculated M_n of PE-*block*-P*t*BA was 11 000, and the weight ratio of a polyethylene segment in PE-*block*-P*t*BA was 6.8%.

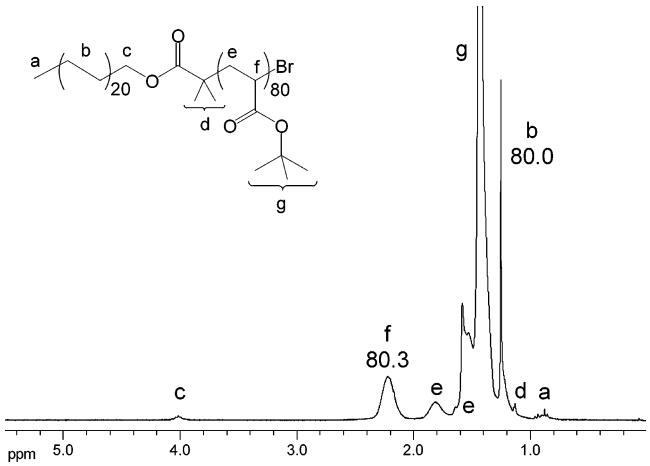

Figure 8. ^{1}H NMR spectrum of PE-*block*-P*t*BA in $CDCl_3$ at 30 °C (300 MHz).

Scheme 6. Preparation of PBA-*graft*-PE via ATRP

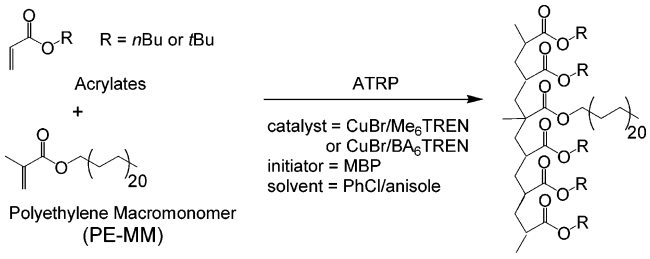

Preparation of Poly(butyl acrylate)s-*graft*-polyethylene via ATRP. Graft copolymers with linear polyethylene side chains such as poly(*n*-butyl acrylate)-*graft*-polyethylene are seldom reported due to the difficulty of efficiently synthesizing a polyethylene macromonomer (PE-MM). One example of a hyperbranched PE-MM synthesis involved a di(imino)palladium complex as a catalyst for living polymerization (one Pd catalyst for each PE-MM chain).[58] In contrast, DT coordination ethylene polymerization produces hundreds of PE-MMs with low polydispersity from only one active Fe catalyst in the presence of the degenerative chain transfer agent $ZnEt_2$.

Grafting-through ATRP of butyl acrylates with the PE-MM led to graft copolymers with poly(butyl acrylate) backbones and polyethylene side chains (Scheme 6). The reaction conditions are summarized in Table 3. Cu(I) complexes with either BA_6TREN or Me_6TREN ligand were used as the catalysts. Chlorobenzene (70 vol %) was used as solvent to dissolve copper catalyst, PE-MM, and the resulting graft copolymers.

The first-order kinetic plots for copolymerization of BA with PE-MM are shown in Figure 9. For $[n\text{BA}]_0/[\text{PE-MM}]_0 = 300/5$ (run 1 in Table 3), BA_6TREN was used as a ligand, and the kinetic plot showed some curvature. The first-order kinetic plot was linear with the Cu(I)/Me_6TREN complex.

The evolution of molecular weight with conversion was examined by GPC, and bimodal peaks were observed in all cases, as shown in Figure 10. The peak area of the lower molecular weight polymer progressively decreased with time, and the peak position stayed at the same molecular weight, as expected for the macromonomer. The higher molecular weight peak continuously shifted toward the higher molecular region, and peak area increased with time. Thus, higher molecular weight peak corresponds to a graft copolymer.

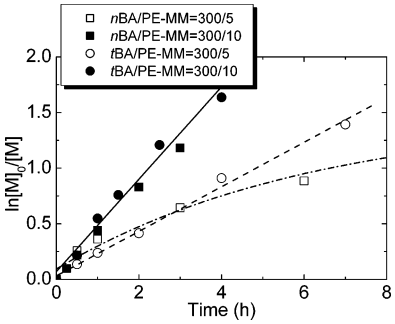

Figure 9. Kinetic plots for copolymerization of BA with PE-MM at 100 °C. See Table 3 for the polymerization conditions.

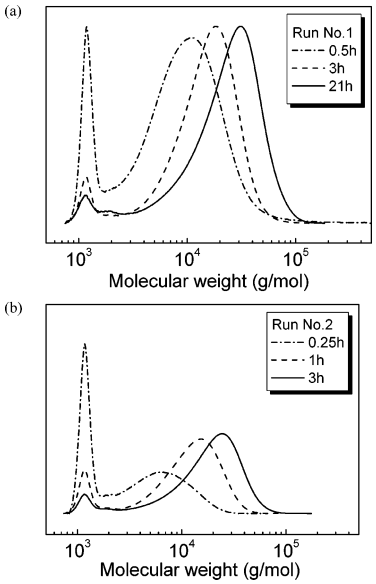

Figure 10. GPC traces for copolymerization of *n*BA with PE-MM (a) $[n\text{BA}]_0/[\text{PE-MM}]_0 = 300/5$ and (b) $[n\text{BA}]_0/[\text{PE-MM}]_0 = 300/10$ through ATRP. See Table 3 for the polymerization conditions.

The evolution of molecular weight for graft copolymers was investigated after eliminating the lower molecular weight peaks by deconvolution of GPC traces. As shown in Figure 11a, for *n*BA, M_n of the graft copolymer increased linearly with *n*BA conversion, and the polydispersity index was low, $M_w/M_n < 1.5$, suggesting that copolymerization was well-controlled. With *t*BA, the plots of number-averaged molecular weight as a function of *t*BA conversion displayed some curvature at higher *t*BA conversion (Figure 11b). The polydispersity of the graft copolymer was $M_w/M_n < 1.5$, as for *n*BA, indicating a well-controlled copolymerization.

After stopping the copolymerization reaction, the remaining unreacted PE-MM was removed from resulting polymer sample by fractionation. Acetone was a suitable solvent for this separation process because PE-MM has poor solubility in acetone, whereas the graft copolymer dissolved in acetone. The molecular weight of the pure graft copolymer was examined by GPC analysis and confirmed the efficient fractionation (Figure 12). Most of the unreacted PE-MM was removed by fractionation, especially for P*t*BA-*graft*-PE because of the better solubility of this copolymer in acetone, as compared to P*n*BA-*graft*-PE. The peak maximum for the graft copolymer shifted toward high molecular weight region after fractionation in both cases.

The molecular structure of the graft copolymer was characterized by ^{1}H NMR spectroscopy after fraction-

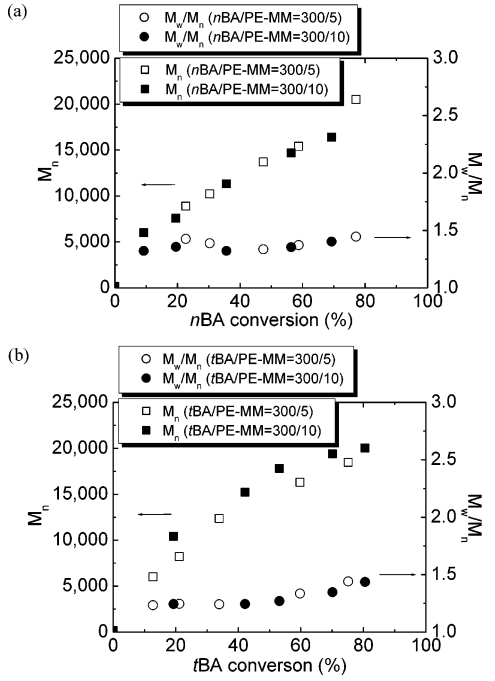

Figure 11. Evolution of M_n and M_w/M_n as a function of BA conversion for copolymerization of (a) *n*BA with PE-MM and (b) *t*BA with PE-MM via ATRP at 100 °C.

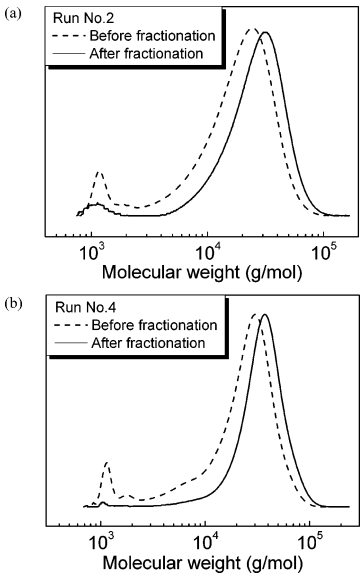

Figure 12. GPC traces before and after fractionation for (a) P*n*BA-*graft*-PE ($[n\text{BA}]_0/[\text{PE-MM}]_0$ = 300/10) and (b) P*t*BA-*graft*-PE ($[t\text{BA}]_0/[\text{PE-MM}]_0$ = 300/10). See Table 3 for the polymerization conditions.

ation. As shown in Figure 13, in the case of P*n*BA-*graft*-PE (run 2 in Table 3), a characteristic singlet of the methylene protons in PE-MM units (δ = 1.25 ppm, peak *m*) could be observed. The degree of polymerization of PE-MM was estimated by comparison of integral for the signal from methoxy protons in the initiator (δ = 3.65 ppm, peak *a*) with signal from the methylene protons in the PE-MM (peak *m*). When the integral for initiator (I_{CH_3O} = 3.0) was taken as corresponding to one end group, the integral from methylene protons in PE-MM (I_{CH_2} = 372) corresponded to 78 protons in the chain with DP = 19.5. Thus, the ratio of PE-MM to the initiator corresponded to ~4.8 grafts per chain (= 372/78). The degree of polymerization of *n*BA was calculated by comparing the integral for the methoxy protons in the

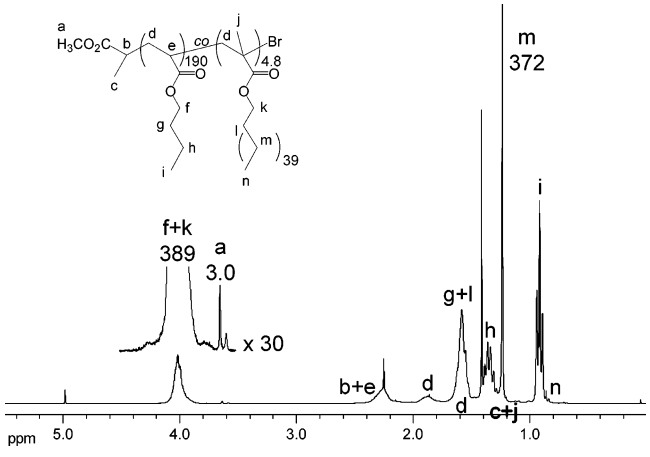

Figure 13. ^{1}H NMR spectrum of P*n*BA-*graft*-PE in $CDCl_3$ at 30 °C (300 MHz).

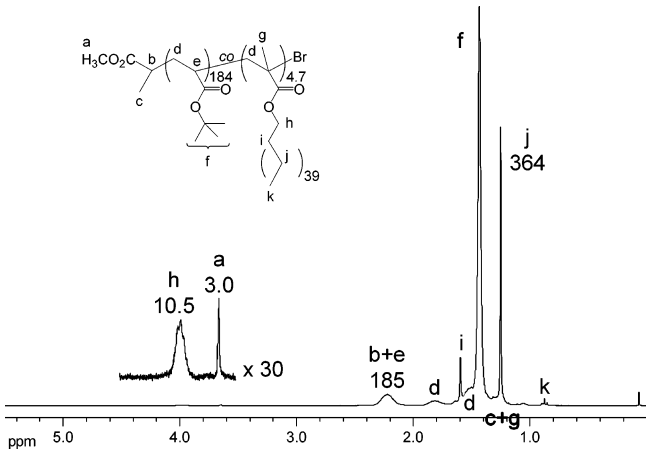

Figure 14. ^{1}H NMR spectrum of P*t*BA-*graft*-PE in $CDCl_3$ at 30 °C (300 MHz).

initiator (δ = 3.65 ppm, peak *a*) with the integral for the signal due to the methylene protons next to the oxygen atom in *n*BA and PE-MM (δ = 4.0 ppm, peak *f* + *k*). The integral for these methylene protons (I_{CH_2O} = 389) corresponded to 194.5 units of methylene groups when the integral of an initiator (I_{CH_3O} = 3.0) corresponded to one unit. Since this integral also included the signal from 4.8 units of PE-MM, the ratio of *n*BA to an initiator was ≈190. Accordingly, the average number of *n*BA units and PE-MM units in graft copolymer were 190 and 4.8, respectively.

The ^{1}H NMR spectrum of P*t*BA-*graft*-PE (run 4 in Table 3) is shown in Figure 14. The singlet peak derived from methylene protons in PE-MM units (δ = 1.25 ppm, peak *j*) is present, as in the P*n*BA-*graft*-PE. Methylenoxy protons in PE-MM (δ = 4.0 ppm, peak *h*) emerge as an isolated peak. The degree of polymerization of PE-MM was estimated on the basis of the integral of the methoxy protons in the initiator (δ = 3.65 ppm, peak *a*, *I* = 3.0) and the integral for the methylene protons (peak *j*, *I* = 364) and the value determined DP_{PE-MM} = 4.7 (= 364/78). This agree well with the value DP_{PE-MM} = 5.3, derived from comparison of integrals of peaks *a* and *h*. The degree of polymerization of *t*BA was calculated on the basis of the integral of methoxy protons in an initiator (peak *a*, *I* = 3.0) and the integral of methine proton in *t*BA unit and an initiator (δ = 2.2 ppm, peak *b* + *e*, *I* = 185). Since the integral of methine proton included one initiator unit, the DP_{tBA} was determined to 184. Then, the calculated M_n of the graft copolymer

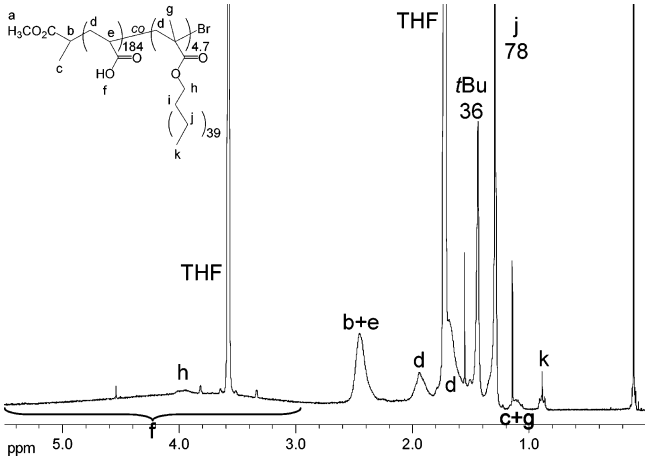

Figure 15. ^{1}H NMR spectrum of PAA-*graft*-PE in THF-d_8 at 30 °C (300 MHz).

was compared to the M_n measured by GPC (Table 3). It should be noted that the integral for initiator may not be very accurate because of the small peak area and low sensitivity of this chain end under this measurement condition. Moreover, these graft copolymers may form aggregated assembly like micelle in the polar solution. Accordingly, they can cause differences of M_n between NMR values and GPC values

Preparation of PAA-*graft*-PE. Hydrolysis of the *t*Bu ester groups in the P*t*BA-*graft*-PE copolymer provided an amphiphilic polymer composed of a poly(acrylic acid) backbone with PE side chains. Hydrolysis was achieved by using 5 equiv of trifluoroacetic acid to *t*Bu ester groups in the P*t*BA-*graft*-PE (run 4 in Table 3). The reaction mixture turned heterogeneous after 15 h hydrolysis in CH_2Cl_2, and the precipitated PAA-*graft*-PE solid was collected. The molecular structure of this solid was investigated by ^{1}H NMR spectroscopy in deuterated THF (Figure 15). The presence of several peaks from the PE-MM (e.g., peaks *h*, *j*, and *k*) proved that the PE side chains still resided in the graft copolymer after hydrolysis. A small singlet peak for *t*Bu ester groups (δ = 1.45 ppm) and a broad peak from the carboxylic acid groups (δ = 3.0−5.5 ppm, peak *f*) could be observed, suggesting incomplete conversion. The extent of hydrolysis was determined by a comparison of the integral from the methylene proton in PE-MM (δ = 1.25 ppm, peak *j*, I_{CH_2} = 78) with the integral from the *t*Bu ester group (I_{tBu} = 36). The units of *t*Bu ester groups in the PAA-*graft*-PE corresponded to 4 times larger than that of PE-MM (4.7 units per a chain). Thus, the degree of polymerization of remaining P*t*BA units was 18.8 in the PAA-*graft*-PE. This could indicate that the carboxylic acid functionality in the PAA-*graft*-PE was 90% (= (184 − 18.8)/184). The micellization of the partially hydrolyzed copolymer does not allow the quantitative conversion of hydrolysis.

DSC Analysis of Graft Copolymers with PE Side Chains. Graft copolymers such as PBA-*graft*-PE and PAA-*graft*-PE consist of an amorphous backbone and crystalline side chains. Therefore, the phase separation and structure of these graft copolymers could be investigated by DSC. The DSC traces for the P*n*BA-*graft*-PE are shown in Figure 16a. A mixture of poly(*n*BA) (DP = 196, prepared by ATRP) and PE-MM (DP_{PE} = 20) was used as a reference sample. The T_g derived from *n*BA and T_m derived from PE-MM were recorded at −47.3 °C and 81.1 °C, respectively. The two T_g's that appeared

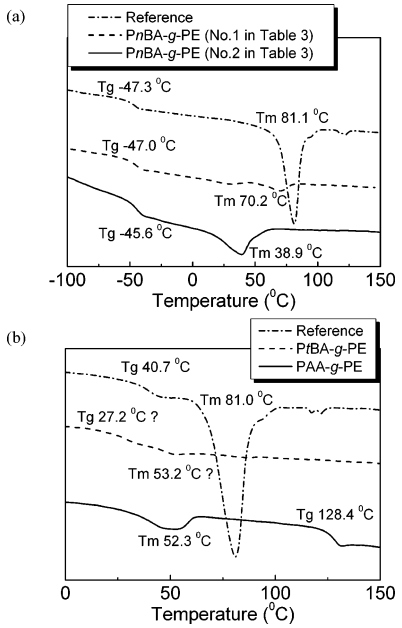

Figure 16. DSC traces for (a) P*n*BA-*graft*-PE and (b) P*t*BA-*graft*-PE and PAA-*graft*-PE.

in the graft copolymers gave almost the same value as that of poly(*n*BA). In contrast, the two T_m values for PE side chains were lower than 81 °C in both cases. This gives additional evidence for incorporation of PE-MM into the graft copolymers and their partial miscibility. Shift in the T_m peak implied that the crystallinity of the PE side chains was lower than in PE-MM and indicated that the neighboring poly(*n*BA) backbone might suppress the crystallization of PE side chains. Figure 16b shows the DSC traces for mixture of poly(*t*BA) (DP = 131, prepared by ATRP) and PE-MM (DP_{PE} = 20) as a reference sample. The T_g for poly(*t*BA) and T_m for PE-MM were 40.7 °C and 81.0 °C, respectively. Surprisingly, neither the T_g peak nor the T_m peak was clearly observed in the case of the P*t*BA-*graft*-PE copolymer presumably due to the poor phase separation. However, a broad T_m peak (52.3 °C) and a new T_g peak corresponding to PAA (128.4 °C) were observed for PAA-*graft*-PE, indicating phase-separated morphology in this graft copolymer and indicating efficient transformation to acrylic acid functionalities.

Conclusions

DT coordination ethylene polymerization catalyzed by a MAO-activated bis(imino)pyridine−iron complex in the presence of the chain transfer agent $ZnEt_2$ was successfully used to form low-polydispersity PE. This PE was converted by oxidation and hydrolysis to PE-OH and further transformed to PE-MI and to PE-MM, which find potential application in industrial processes. The PE-MI and PE-MM were used to prepare block and graft copolymers with precise molecular structures via ATRP. These synthetic procedures are important for tuning the chemical and physical properties of polyethylene segmented copolymers with block and graft morphology, and increasing their precision will require further investigation.

Acknowledgment. We greatly appreciate the financial support from the National Science Foundation (DMR-0090409 and CHE-0130903), Mitsui Chemicals,

Inc., and CRP Consortium at Carnegie Mellon University.

References and Notes

(1) Ziegler, K.; Holzkamp, E.; Breil, H.; Martin, H. *Angew. Chem.* **1955**, *67*, 541.
(2) Natta, G.; Pino, P.; Corradini, P.; Danusso, F.; Mantica, E.; Mazzanti, G.; Moraglio, G. *J. Am. Chem. Soc.* **1955**, *77*, 1708.
(3) Kashiwa, N. *J. Polym. Sci., Part A: Polym. Chem.* **2004**, *42*, 1.
(4) Sinn, H.; Kaminsky, W.; Vollmer, H. J.; Woldt, R. *Angew. Chem., Int. Ed. Engl.* **1980**, *19*, 390.
(5) Coates, G. W. *Chem. Rev.* **2000**, *100*, 1223.
(6) Brintzinger, H. H.; Fischer, D.; Muelhaupt, R.; Rieger, B.; Waymouth, R. M. *Angew. Chem., Int. Ed. Engl.* **1995**, *34*, 1143.
(7) Britovsek, G. J. P.; Gibson, V. C.; Wass, D. F. *Angew. Chem., Int. Ed.* **1999**, *38*, 428.
(8) Gibson, V. C.; Spitzmesser, S. K. *Chem. Rev.* **2003**, *103*, 283.
(9) Ittel, S. D.; Johnson, L. K.; Brookhart, M. *Chem. Rev.* **2000**, *100*, 1169.
(10) Britovsek, G. J. P.; Bruce, M.; Gibson, V. C.; Kimberley, B. S.; Maddox, P. J.; Mastroianni, S.; McTavish, S. J.; Redshaw, C.; Solan, G. A.; Stroemberg, S.; White, A. J. P.; Williams, D. J. *J. Am. Chem. Soc.* **1999**, *121*, 8728.
(11) Scollard, J. D.; Mcconville, D. H. *J. Am. Chem. Soc.* **1996**, *118*, 10008.
(12) Wang, C.; Freidrich, S.; Younkin, T. R.; Li, R. T.; Grubbs, R. H.; Bansleben, D. A.; Day, M. W. *Organometallics* **1998**, *17*, 3149.
(13) Matsui, S.; Mitani, M.; Saito, J.; Tohi, Y.; Makio, H.; Tanaka, H.; Fujita, T. *Chem. Lett.* **1999**, 1263.
(14) Matsui, S.; Tohi, Y.; Mitani, M.; Saito, J.; Makio, H.; Tanaka, H.; Nitabaru, M.; Nakano, T.; Fujita, T. *Chem. Lett.* **1999**, 1065.
(15) Mitani, M.; Mohri, J.; Yoshida, Y.; Saito, J.; Ishii, S.; Tsuru, K.; Matsui, S.; Furuyama, R.; Nakano, T.; Tanaka, H.; Kojoh, S.-i.; Matsugi, T.; Kashiwa, N.; Fujita, T. *J. Am. Chem. Soc.* **2002**, *124*, 3327.
(16) Mitani, M.; Furuyama, R.; Mohri, J.; Saito, J.; Ishii, S.; Terao, H.; Nakano, T.; Tanaka, H.; Fujita, T. *J. Am. Chem. Soc.* **2003**, *125*, 4293.
(17) Tian, J.; Hustad, P. D.; Coates, G. W. *J. Am. Chem. Soc.* **2001**, *123*, 5134.
(18) Gottfried, A. C.; Brookhart, M. *Macromolecules* **2001**, *34*, 1140.
(19) Baumann, R.; Davis, W. M.; Schrock, R. R. *J. Am. Chem. Soc.* **1997**, *119*, 3830.
(20) Jayaratne, K. C.; Sita, L. R. *J. Am. Chem. Soc.* **2000**, *122*, 958.
(21) Tshuva, E. Y.; Goldberg, I.; Kol, M. *J. Am. Chem. Soc.* **2000**, *122*, 10706.
(22) Coates, G. W.; Hustad, P. D.; Reinartz, S. *Angew. Chem., Int. Ed.* **2002**, *41*, 2236.
(23) Busico, V.; Cipullo, R.; Friederichs, N.; Ronca, S.; Togrou, M. *Macromolecules* **2003**, *36*, 3806.
(24) Gottfried, A. C.; Brookhart, M. *Macromolecules* **2003**, *36*, 3085.
(25) Mitani, M.; Mohri, J.-i.; Furuyama, R.; Ishii, S.; Fujita, T. *Chem. Lett.* **2003**, *32*, 238.
(26) Xu, G.; Chung, T. C. *J. Am. Chem. Soc.* **1999**, *121*, 6763.
(27) Fu, P.-F.; Marks, T. J. *J. Am. Chem. Soc.* **1995**, *117*, 10747.
(28) Shiono, T.; Yoshida, K.; Soga, K. *Makromol. Chem., Rapid Commun.* **1990**, *11*, 169.
(29) Han, C. J.; Lee, M. S.; Byun, D.-J.; Kim, S. Y. *Macromolecules* **2002**, *35*, 8923.
(30) Chung, T. C. *Prog. Polym. Sci.* **2002**, *27*, 39.
(31) Yanjarappa, M. J.; Sivaram, S. *Prog. Polym. Sci.* **2002**, *27*, 1347.
(32) Matyjaszewski, K., Ed. *Controlled Radical Polymerization;* ACS Symposium Series Vol. 685; American Chemical Society: Washington, DC, 1998.
(33) Matyjaszewski, K., Ed. *Controlled/Living Radical Polymerization. Progress in ATRP, NMP, and RAFT*; ACS Symposium Series Vol. 768; American Chemical Society: Washington, DC, 2000.
(34) Matyjaszewski, K., Davis, T. P., Eds. *Handbook of Radical Polymerization*; Wiley-Interscience: Hoboken, 2002.
(35) Matyjaszewski, K., Ed. *Advances in Controlled/Living Radical Polymerization.* ACS Symposium Series Vol. 854; American Chemical Society: Washington, DC, 2003.
(36) Hawker, C. J.; Bosman, A. W.; Harth, E. *Chem. Rev.* **2001**, *101*, 3661.
(37) Wayland, B. B.; Poszmik, G.; Mukerjee, S. L.; Fryd, M. *J. Am. Chem. Soc.* **1994**, *116*, 7943.
(38) Wang, J.-S.; Matyjaszewski, K. *Macromolecules* **1995**, *28*, 7901.
(39) Wang, J.-S.; Matyjaszewski, K. *J. Am. Chem. Soc.* **1995**, *117*, 5614.
(40) Patten, T. E.; Xia, J.; Abernathy, T.; Matyjaszewski, K. *Science (Washington, D.C.)* **1996**, *272*, 866.
(41) Matyjaszewski, K.; Xia, J. *Chem. Rev.* **2001**, *101*, 2921.
(42) Gaynor, S. G.; Wang, J.-S.; Matyjaszewski, K. *Macromolecules* **1995**, *28*, 8051.
(43) Chiefari, J.; Rizzardo, E. In *Handbook of Radical Polymerization*; Matyjaszewski, K., Davis, T. P., Eds.; Wiley-Interscience: Hoboken, 2002; p 629.
(44) Samsel, E. G. In Eur. Pat. Appl. (Ethyl Corp.); EP, 1993; p 13.
(45) Samsel, E. G.; Eisenberg, D. C. In Eur. Pat. Appl. (Ethyl Corp.); EP, 1993; p 12.
(46) Pelletier, J.-F.; Mortreux, A.; Olonde, X.; Bujadoux, K. *Angew. Chem., Int. Ed. Engl.* **1996**, *35*, 1854.
(47) Rogers, J. S.; Bazan, G. C. *Chem. Commun.* **2000**, 1209.
(48) Bazan, G. C.; Rogers, J. S.; Fang, C. C. *Organometallics* **2001**, *20*, 2059.
(49) Mani, G.; Gabbai, F. P. *Angew. Chem., Int. Ed.* **2004**, *43*, 2263.
(50) Britovsek, G. J. P.; Cohen, S. A.; Gibson, V. C.; Maddox, P. J.; Van Meurs, M. *Angew. Chem., Int. Ed.* **2002**, *41*, 489.
(51) Britovsek, G. J. P.; Cohen, S. A.; Gibson, V. C.; Meurs, M. v. *J. Am. Chem. Soc.* **2004**, *126*, 10701.
(52) Zhang, Y.; Keaton, R. J.; Sita, L. R. *J. Am. Chem. Soc.* **2003**, *125*, 9062.
(53) Matyjaszewski, K.; Patten, T. E.; Xia, J. *J. Am. Chem. Soc.* **1997**, *119*, 674.
(54) Gromada, J.; Matyjaszewski, K. *Polym. Prepr.* **2002**, *43*, 195.
(55) Xia, J.; Gaynor, S. G.; Matyjaszewski, K. *Macromolecules* **1998**, *31*, 5958.
(56) Goto, A.; Fukuda, T. *Prog. Polym. Sci.* **2004**, *29*, 329.
(57) Muehlebach, A.; Rime, F. *J. Polym. Sci., Part A: Polym. Chem.* **2003**, *41*, 3425.
(58) Hong, S. C.; Jia, S.; Teodorescu, M.; Kowalewski, T.; Matyjaszewski, K.; Gottfried, A. C.; Brookhart, M. *J. Polym. Sci., Part A: Polym. Chem.* **2002**, *40*, 2736.

MA050263J